Data Repository 2010089

Supplementary Information on the Solution of the Reynolds Equation, Sediment Compaction, and the Finite Element Model

Derivation, and Outline of the Solution, of Reynolds Equation for Salt Flow in a Channel

The theory of the development of VPR's is based on lubrication theory for creeping flow of viscous salt in channels. Assuming lubrication theory approximations (Pozrikidis, 2001), the creeping flux of salt in a 1D channel of uniform thickness h_s containing incompressible salt, viscosity η, density ρ_s, and driven by uniform motion of the sediment overburden at velocities V_1 and V_2 on either side of a convergent pressure ridge width $2L$ (Fig. 2C) is

$$Q(x,t) = Q_C + Q_P = \frac{(V_1 - V_2)h_s}{2} - \frac{h_s^3}{12\eta}\frac{\partial p(x,t)}{\partial x}. \qquad \text{(DR1)}$$

When the pressure driving Q_P is caused by the excess height of the salt, $p(x,t) = \rho_s g h(x,t)$, it follows that $Q_P = -k\partial h/\partial x$, where $k = \rho_s g h_s^3/12\eta$. If sediment, average density $\bar{\rho}_0$, fills the minibasin accommodation space above the channel to the maximum height of the pressure ridge $h(0,t)$, the same equation applies but $k = (\rho_s - \bar{\rho}_0) g h_s^3/12\eta$. Using the continuity equation, $\partial Q(x,t)/\partial x + \partial h(x,t)/\partial t = 0$, and substituting into equation DR1 gives

$$k\frac{\partial^2 h(x,t)}{\partial x^2} + S(x,t) = \frac{\partial h(x,t)}{\partial t}. \qquad \text{(DR2)}$$

This is Reynolds equation for a constant channel conductivity, k, and a salt source term $S(x,t) = \Delta V h_s D(x)/4L$. It is nonlinear when $k = k(x,t)$ (equation 1). $S(x,t)$ is derived from $(\partial/\partial x)(V_1 - V_2)h_s/2$, the salt production per unit ridge length across the pressure ridge, width $2L$, assuming a uniform Couette velocity gradient across the ridge. $D(x)$ is the unit height boxcar function between $-L$ and $+L$.

The basic form of the equation is solved for the balance between the production of salt $S(x,t)$ in the pressure ridge, as a result of differential Couette flow, and the diffusion of salt out of the ridge by Poiseuille flow. The solution of the basic Reynolds equation (equation DR2) for constant channel conductivity, $k = (\rho_s - \overline{\rho}_0) g h_s^3 / 12\eta = const.$ and initial conditions, $h(x,0) = 0$, is constructed using the space-time Green function approach (Özişik, 1980). The problem in which $S(x,t)$ is an initial delta function, is solved first, and its solution is then convolved with the distributed salt production rate $S(x,t) = S_c D(x)$, where $S_c = \Delta V h_s / 4L$.

The definite solution for salt production between $t = 0$ and $t = \tau$ is

$$h(x,t) = \frac{S_c}{4k} \left\{ L_-^2 \left(\frac{erf(\beta L_-)}{2\beta L_-} + \frac{e^{-\beta^2 L_-^2}}{\beta L_- \sqrt{\pi}} + erf(\beta L_-) \right) - L_+^2 \left(\frac{erf(\beta L_+)}{2\beta L_+} + \frac{e^{-\beta^2 L_+^2}}{\beta L_+ \sqrt{\pi}} + erf(\beta L_+) \right) \right\} \Bigg|_{\beta=\frac{1}{\sqrt{4kt}}}^{\infty} \tag{DR3}$$

where *h(x,t)*, is the excess height of the base of the minibasins/top of the salt channel with respect to the initial salt thickness, and *erf* is the error function. $L_+ = l + x$, $L_- = l - x$, and $\beta = \dfrac{1}{2\sqrt{k(t-\tau)}}$.

This solution for a fixed width source that is constant in space and time forms the basis for time stepping the evolving system. The full solution, calculated using *Maple 11*^{TM}, (www.maplesoft.com) involves four modifications noted in the text.

The evolution of the system is calculated by incremental time steps. Each time step, *i,* starting at t_i and of duration Δt, involves the following computations.

i) Calculate the incremental basic solution of the Reynolds equation for constant k_I comprising the following parts.

i-a) Relaxation of $h(x,t_i)$ for Δt by convolving the pressure distribution, $\rho_{os} g h(x,t_i)$ with the space Green function. This represents the pumping effect of the salt pressure ridge and sediments on the existing salt. For this computation the sediments act with their surface uncompacted density, ρ_{os}, and the configuration is that at t_i.

i-b) Growth of the pressure ridge during the time step using the midpoint model configuration, midpoint pressure ridge boxcar width $D(x,t_i + \Delta t/2)$ and midpoint salt production rate $S_c(t_i + \Delta t/2)$. This step is iterated to improve the calculated midpoint configuration.

ii) Correct the basic solution for the incremental redistribution effects of evolving channel thickness and sediment compaction by convolving the redistribution terms, based on the midpoint geometry, with the space-time Green function. This correction is also iterated using successively improved estimates of the midpoint configuration.

iii) Update the geometry of the system, $h(x,t)$ at $t_i + \Delta t$ for the effects of horizontal advection including pressure ridge narrowing and floe translation.

To grow minibasins successfully, the VPR mechanism must achieve the R-T instability threshold in a time, $\tau_{R\text{-}T}$, that is less than that required to close the pressure ridge. $\tau_{R\text{-}T}$ depends on channel conductivity $k = (\rho_s - \overline{\rho}_0) g h_s^3 / 12\eta$, initial pressure ridge width L, differential Couette flux $\Delta V h_s$, and the critical sediment thickness at which $\overline{\rho}_o(x,t) = \rho_s$ (1700 m for Gulf of Mexico sediment compaction).

Supplementary Information on Sediment Compaction and Density Distribution

We calculate the sediment density from $\rho_0 = \rho_{gr} - (\rho_{gr} - \rho_w)\phi$, where ρ_{gr} is the grain density, ρ_w is the density of the interstitial water and ϕ is the porosity, and assume that the porosity decreases exponentially (Athy, 1930) with depth from its surface value ϕ_0 with compaction coefficient α. Under these circumstances, the vertically averaged density of sediment in the minibasin is

$$\overline{\rho}_0(x,t) = \rho_{gr} - (\rho_{gr} - \rho_w)\phi_0 \exp(-\alpha h_{MB}(x,t) - 1) / \alpha h_{MB}(x,t), \qquad \text{(DR4)}$$

where $h_{MB}(x,t) = h(0,t) - h(x,t)$ is the thickness of the sediment in the minibasin, assuming filling to the top of the pressure ridges. The perturbation of the sediment density with respect to the surface value is $\Delta\overline{\rho}_0(x,t) = \overline{\rho}_0(x,t) - \rho_{os}$. $\Delta\overline{\rho}_0(x,t)$, and its spatial derivatives, are required in the space-time convolutions for the salt redistribution.

We have used sediment compaction parameters corresponding to observations from the Gulf of Mexico (Fig. DR2, see also Hudec et al., 2009) and for these values the Rayleigh-Taylor threshold occurs when the sediment thickness is 1700 m.

Supplementary Information on the Finite Element Model

The finite element model (Fig. 5) represents a 50 km wide plane strain region comprising a 1 km thick layer of salt (magenta), viscosity 10^{18} Pa s, overlain by two laterally tapering layers of frictional plastic overburden (yellow). The overburden has an effective internal angle of friction, $\phi_{eff} = 20°$. There is no overburden in the central region of the model. The top of the model is a nearly flat free surface and the overburden is in equilibrium floating in the salt. The lateral velocity boundary conditions are V= +/- 1 cm a^{-1} at the surface and within the overburden, with velocity decreasing linearly to $V = 0$ at the base of the model. The base is a no-slip boundary.

The finite element model solves the equations for incompressible creeping flow;

$$\frac{\partial \sigma_{ij}}{\partial x_i} - \frac{\partial P}{\partial x_j} + \rho g = 0 \qquad i,j = 1,2, \qquad \text{(DR5)}$$

$$\frac{\partial v_i}{\partial x_i} = 0 \qquad i=1,2, \qquad \text{(DR6)}$$

where σ_{ij} is the deviatoric stress tensor, x_i are the spatial coordinates, P pressure, ρ density, g gravitational acceleration, and v_i the components of velocity.

The velocity field, strain rate, deformation, and stress, subject to specified velocity boundary conditions, are calculated using an Arbitrary Lagrangian Eulerian (ALE) methodology, which solves large-deformation flows with free upper surfaces on an Eulerian finite-element grid that stretches vertically to conform to the material domain. A Lagrangian grid and passive tracking particles, advected with the model velocity field, are used to update the mechanical and thermal property distributions on the Eulerian grid.

Model materials have either frictional-plastic (brittle) or linearly viscous (Newtonian) properties. Drucker-Prager frictional-plastic yielding of the overburden occurs when

$$(J_2')^{1/2} = C\cos\phi_{eff} + P\sin\phi_{eff} \quad \text{(DR7)}$$

where J_2' is the second invariant of the deviatoric stress, P the dynamical pressure (mean stress), and C the cohesion. The effective internal angle of friction, ϕ_{eff}, is defined to include the effects of pore fluid pressures through the approximate relation

$$P\ sin\phi_{eff} = (P- P_f)\ sin\phi_d \quad \text{(DR8)}$$

where ϕ_d is the internal angle of friction for dry conditions ($P_f = 0$) and P_f is pore fluid pressure.

Sediment is added to the surface of the model each time step so that the level of the horizontal surface is 10 m below the top of the pressure ridge. The density of the sediment at the surface is 1900 kg m^{-3} and it compacts with depth of burial according to the exponential compaction (see above and Figure DR1).

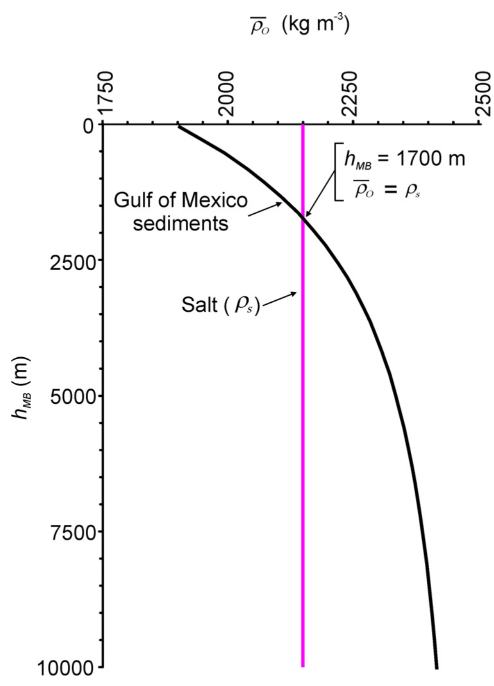

Figure DR1. Exponential density versus depth compaction curve (black) used in the calculations based on Gulf of Mexico compaction curves (Jackson and Talbot, 1986) compared with the density of halite (magenta). Compaction parameters used to generate the black curve are as follows: ρ_w = 1000 kg m^{-3}, ρ_{gr} = 2500 kg m^{-3}, ϕ_0 = 0.40, and α = 0.70 km^{-1}.

References

Athy, L.F., 1930, Density, porosity, and compaction of sedimentary rocks: American Association Petroleum Geologists Bulletin, v. 14, p. 1-24.

Hudec, M.R., Jackson, M.P.A., and Schultz-Ela, D.D., 2009, The paradox of minibasin subsidence into salt: clues to the evolution of crustal basins. Geological Society America Bulletin, doi:10.1130/B26275.1.

Jackson, M.P.A., and Talbot, C.J., 1986, External shapes,strain rates, and dynamics of salt structures: Geological Society of America Bulletin, v. 97, p. 305–323.

Maple 11™, www.maplesoft.com, Maplesoft™

Özişik, M.N., 1980, Heat Conduction, John Wiley and Sons, New York, 687pp.

Pozrikidis, C., 2001, Fluid Dynamics - Theory, Computation and Numerical Simulation, Springer-Verlag, 675 pp.